Spectral Characteristics of Rotor Blade/Vortex Interaction Noise

Ruth M. Martin* and Jay C. Hardin†
NASA Langley Research Center, Hampton, Virginia

The blade/vortex interaction (BVI) impulsive content of a rotor acoustic signal is shown to appear in the mid-frequency range of the power spectrum, between the 5th and 30th harmonics of the blade passage frequency, concentrated at the harmonics of the blade passage frequency. These harmonics exhibit a humped or scalloped shape in this midfrequency spectral region. Increased energy at the harmonics of the shaft frequency appears when the BVI impulsive content demonstrates unsteadiness and blade-to-blade differences in the time domain. The experimental data are interpreted via a mathematical model of a generalized BVI acoustic signal and its power spectrum. This model shows that the power spectrum is scalloped and filtered by a comb function, with the amplitude defined by the impulse amplitude and emission time. The scalloping of the spectrum is related to the emission time of the impulse itself and the spacing of the comb function is related to the repetition time (period) of the impulse. The decay rate of the spectral humps is governed by the inverse of frequency squared. The mathematical model illustrates the characteristics observed in the data and implies that these characteristics are due to blade/vortex interaction activity.

Nomenclature

A	= peak amplitude of BVI impulse, dynes/cm^2
B_0	= arbitrary constant
BVI	= blade/vortex interaction
C_t	= rotor thrust coefficient
f	= frequency, Hz
f_{bpf}	= rotor blade passage frequency, number of rotor blades times rotor rotational speed, 92 Hz
P	= repetition time of BVI impulse, s
R	= rotor radius, 4.67 ft
T	= emission time of BVI impulse, s
V	= tunnel speed, knots
X_0	= arbitrary constant
α	= rotor tip-path-plane angle, deg
μ	= rotor tip speed ratio, $V/\Omega R$
ψ	= rotor blade azimuth angle, zero over tail, deg
ω	= frequency, rad/s
Ω	= rotor rotational speed, 145 rad/s

Introduction

A GREAT deal of research in recent years has been devoted to the study of rotor blade/vortex interaction (BVI) noise. In both experimental and analytical work, the emphasis has been on the temporal characteristics of the phenomenon. Quantification of rotor BVI impulsive activity is difficult, as there is at present no precise definition of a BVI acoustic impulse other than each researchers' subjective assessment of the acoustic signal. Rotor BVI acoustic content has been previously quantified using peak-to-peak pressures,[1,2] A-weighted sound levels,[2,3] band-limited sound levels,[4] and general trends in spectral shape.[2,5-7] While the research community acknowledges that increased impulsive activity results in increased harmonic levels in the midfrequencies of a rotor spectrum,[3,8-11] no study investigating the detailed spectral content of BVI noise has been reported thus far.

This work presents the results of a study into the details of the spectral characteristics of a rotor signal containing a strong BVI acoustic impulse, using the acoustic data from a model-scale rotor wind-tunnel experiment. It attempts to increase understanding of the BVI spectral characteristics by relating them to particular aspects of a simple mathematical model. The trends of the blade passage frequency harmonics and subharmonics are considered in conjunction with the averaged and instantaneous acoustic time histories. A mathematical model of a generalized BVI acoustic signal is developed to display the trends observed in the measured data. The model explains the presence of significant acoustic energy at the harmonics of the blade passage frequency and it shows that these harmonics and the general spectral shape are related to the periodicity of the BVI impulses and to the emission time of the BVI impulses. Increased unsteadiness and blade-to-blade differences in the acoustic impulses are shown to lead to a spreading of energy from the blade passage harmonics to the rotor shaft harmonics (the quarter-blade-passage harmonics for this model four-bladed rotor).

Experimental Setup and Data Acquisition

The acoustic data studied herein were acquired during a model-scale rotor acoustics experiment[4] in the NASA Langley 14×22 ft subsonic tunnel (formerly called 4×7 m wind tunnel). The experiment was designed specifically to study rotor blade/vortex interaction noise generation. The tunnel was operated in the open-throat mode (fixed test section floor, with test section sides and top open to the test chamber) and was treated with acoustic foam and absorptive panels to improve its anechoic qualities. The test rotor was a sting-mounted model system that employed a generic fuselage and an electric drive. The rotor was a four-bladed, one-fifth-scale model of a contemporary operational rotor and was mounted on a fully articulated hub. Nineteen ½ in (0.635 cm) free-field condenser microphones were placed in and around the tunnel test section. Data measured at one in-flow near-field location

Presented as Paper 87-0251 at the AIAA 25th Aerospace Sciences Meeting, Reno, NV, Jan. 12-15, 1987; received Feb. 19, 1987; revision received June 12, 1987.

*Research Engineer, Aeroacoustics Branch, Acoustics Division. Associate Member AIAA.

†Senior Research Scientist, Aeroacoustics Branch, Acoustics Division.

will be presented here (microphone 1 from Ref. 4, 2.2 ft from the rotor hub, 35 deg down from the rotor plane, and at 110 deg azimuth angle ψ). The acoustic signals were recorded unfiltered using a frequency-modulated tape recording system that had a useful frequency range of about 20 kHz. Microphone system calibrations were performed using the standard pistonphone method. Further details of the facility, test program, experimental apparatus, data repeatability, signal-to-noise ratio, and a substantial presentation of the performance and acoustic data are provided in Refs. 4 and 12-14.

Acoustic Data Reduction

The analog acoustic signals were digitized using a conditional sampling technique based on the rotor once-per-revolution signal. A synchronizer sampled the acoustic signals at 1024 equally spaced intervals in each rotor revolution and then constantly updated the sample rate to adjust for small changes in the rotor rotational speed. The acoustic time histories of 50 rotor revolutions were sampled and then ensemble averaged to obtain an average acoustic waveform and standard deviation. This averaging technique removes random fluctuations such as background noise and enhances the periodic content of the signal.

To obtain spectra, 200 rotor revolutions were conditionally sampled and the data of four sequential rotor revolutions were transformed to the frequency domain using a 4096 point fast Fourier transform algorithm. This yielded 50 spectra with a bandwidth of 1/16 blade passage frequency. The results of each of these 50 power spectra were then averaged to obtain an average power spectrum. Considering each spectral estimate as a Chi-squared random varible, the statistical accuracy of the spectral results is ± 0.8 dB for an 80% confidence interval.

The power spectra have been corrected for tunnel background noise as a function of tunnel speed. Since the NASA Langley 14 × 22 ft subsonic tunnel is not an anechoic facility, the acoustic data measured therein are contaminated to some extent with acoustic reflections, primarily from the floor of the tunnel test section. The power cepstrum technique[15] was employed to remove the major effects of the reflected signal from the power spectra of the rotor signals. Corrections for background noise or acoustic reflections have not been applied to any of the time history data.

Spectral Characteristics from Experimental Data

Figure 1 presents the averaged time histories plotted vs normalized time (time divided by rotation period) for a near-field microphone (microphone location 1 from Ref. 4). The middle curve is the mean signal, while the upper and lower dashed curves are the standard deviation as a function of time about this mean. This set of measurements was made with a fixed tunnel speed and rotor thrust coefficient ($V=70$ knots, $\mu=0.175$, $C_t=0.0070$), as the rotor was swept through a series of tip-path-plane angles from -4 to 8 deg in 2 deg increments (some of the measurements have been omitted for clarity). The objective of this was to vary the rotor wake trajectory and to move the rotor from ascent (negative angle) through level flight to descent (positive angle) to locate conditions of strong BVI acoustic activity. Very little impulsive content can be seen at -4 deg tip-path-plane angle. The occurrence of BVI acoustic activity is clearly seen at 0, 4, and 6 deg tip-path-plane angle. At 8 deg, the signal becomes nonimpulsive again.

At 6 deg, the mean signal exhibits the sharpest impulsive content. The standard deviation bands clearly follow the distinct shape of the BVI impulses, indicating that the impulse emission times are very repeatable from revolution to revolution, although the impulse amplitudes are not repeatable from revolution to revolution. The mean signals at 0 and 4 deg also show impulsive content, but it is less distinct. Further, the standard deviation bands at 0 and 4 deg are more widely spread about the mean, particularly near the time of BVI impulsive activity. While the impulse emission times appear to be quite steady at 6 deg, there appears to be a significant variability at 0 and 4 deg. Since the standard deviation is large near the impulsive content in the mean signal, this indicates there is also a large variability in impulse amplitude.

Figure 2 presents the instantaneous time histories of one revolution for the same test conditions as Fig. 1. The instantaneous and averaged time histories at -4 deg look much the same. At 0, 4, and 6 deg tip-path-plane angle, the instantaneous time histories are all quite impulsive. The highest impulsive amplitudes are seen at 4 deg. A comparison of the instantaneous and averaged signals suggests that the signals at 0 and 4 deg are quite unsteady, whereas at 6 deg the signal is relatively steady. The instantaneous signal at 8 deg exhibits a low level of impulsive activity, but seems to be represented well by the averaged signal of Fig. 1.

These results illustrate that a subjective assessment of the BVI acoustic activity of a signal based solely on the instantaneous or averaged signal can be misleading. A comparison of the two representations of the signal should be made before any conclusions are drawn about its impulsive content or repeatability.

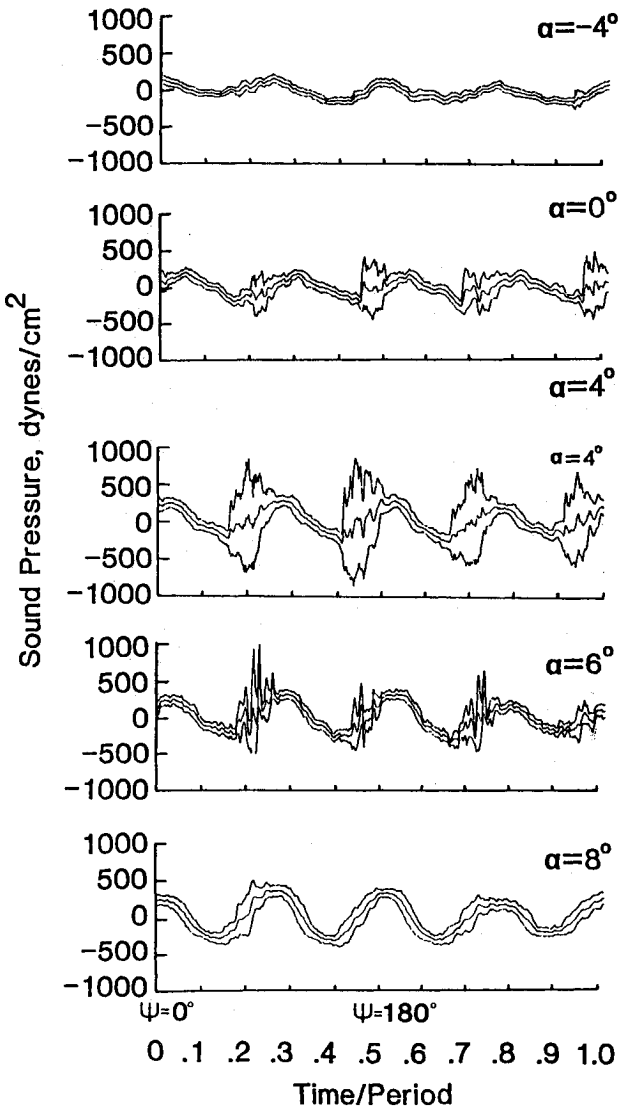

Fig. 1 Mean and standard deviation of averaged acoustic signals for tip-path-plane angle from -4 to 8 deg (50 averages, $V=70$ knots, $C_t=0.0070$, $\mu=0.175$, microphone 1 of Ref. 4).

A large variability in the BVI impulses created by each unique blade is evident in all of these signals. Substantial blade-to-blade differences have been reported in previous studies of BVI noise.[6,7,11] A good example is seen in both the averaged and instantaneous time histories (Figs. 1 and 2) at 6 deg, where the first blade passage shows three BVI impulses, while the second blade passage clearly shows two BVI impulses. These obvious "blade-to-blade" differences may be attributed to several factors, the most important of which is the possibility of differing "track" of the four blades, attributable to slight manufacturing differences (although the rotor was tracked and balanced in hover as part of the pretest procedure). The track differences cause differing vortex sizes, strengths, and trajectories of the tip vortices created by the four blades.

The averaged narrow band spectra for each of these conditions are shown in Fig. 3. The blade passage harmonics (nf_{bpf}, $n=1,2,3,...$) are accented with the solid symbols and the half-blade-passage harmonics with the open symbols (except for those already marked by the solid symbols). The open symbols thus represent the $(n/2)f_{bpf}$ ($n=1,3,5,...$) frequencies. The occurrence of BVI impulses for these data have been found[4] to create increased levels in the spectrum between approximately 500 and 3000 Hz; thus, only this region of the spectrum is presented here. For these data, this corresponds to the region between the 5th and 30th blade passage harmonic. This acoustic power increase may be seen by comparing the spectra measured at -4 and 8 deg, which show little impulsive content in the time domain, with those at 0, 4, and 6 deg. The spectra at -4 and 8 deg exhibit the lowest levels. The spectra of 0, 4, and 6 deg exhibit a humped shape in this midfrequency spectral region, particularly true of the blade passage harmonics at 4 and 6 deg. The humps in the blade passage harmonics appear to be centered around 1000, 1750, and 2500 Hz. The major part of this midfrequency energy appears to be created mainly at harmonics of the blade passage frequency (approximately 90 Hz). However, there is also significant energy in the half- and quarter-blade-passage harmonics (the shaft harmonics). In some cases, particularly at 0 and 4 deg, the half-blade-passage harmonics have equal or higher levels than the blade passage harmonics themselves.

A scalloped shape in a power spectrum can be attributed to the presence of a ground reflection. However, the spectra presented here have been corrected for the major effects of the reflected content using the power cepstrum technique,[15] so this is not considered a likely cause. The energy observed at the subharmonics also cannot be attributed to spectral leakage. The sychronized method of digitization, based on the rotor rotation rate, prevents spectral leakage. In addition, the narrow analysis bandwidth is such that there are 16 spectral calculations between the blade passage harmonics (and 4 spectral calculations between shaft harmonics). Direct leakage from one blade passage harmonic to another is negligible.

Mathematical Model of Blade/Vortex Interaction Impulse

A mathematical model of a simple blade/vortex interaction-type of impulse was considered in an effort to further understand these observed spectral trends. This model is shown in Fig. 4a and can be expressed as

$$
\begin{aligned}
b(t) &= \frac{4At}{T} && \text{for } 0<t<\frac{T}{4} \\
&= \frac{4A}{T}\left(\frac{T}{2}-t\right) && \text{for } \frac{T}{4}<t<\frac{3T}{4} \\
&= \frac{4A}{T}(t-T) && \text{for } \frac{3T}{4}<t<T \\
&= 0 && \text{for } t>T
\end{aligned} \qquad (1)
$$

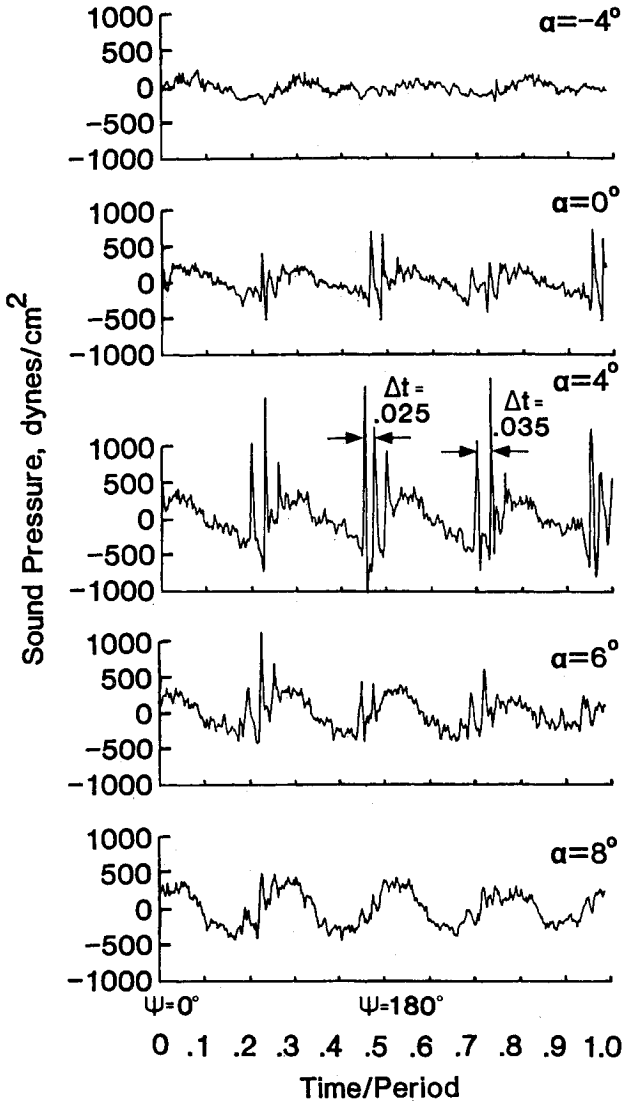

Fig. 2 Instantaneous acoustic signals for tip-path-plane angles from -4 to 8 deg ($V=70$ knots, $C_t=0.0070$, $\mu=0.175$, microphone 1 of Ref. 4).

where A is the peak amplitude and T the impulse emission time. The magnitude of the Fourier transform of this model can be expressed as

$$
|B(\omega)| = \frac{AT}{2\pi}\left|\frac{\sin(\omega T/4)\,[1-\cos(\omega T/4)]}{(\omega T/4)^2}\right| \qquad (2)
$$

and is plotted in decibels [$20\log|B(\omega)|$] plus an arbitrary constant B_0 in Fig. 4b for $A=1.0$, $T=0.0013$ s. This spectrum exhibits a characteristic scalloped shape with center frequencies located very near to

$$
\omega = 2\pi k/T \qquad k=1,3,5...
$$

Thus, the center frequencies of the spectral humps, or maxima, are directly related to the impulse emission time T.

Now, suppose these individual signals occur periodically with period P, as shown in Fig. 5a. This is the situation that would prevail if all of the blades produced exactly the same BVI impulse. Now, the time series may be represented as

$$
f(t) = \sum_{n=-\infty}^{\infty} b(t-nP)
$$

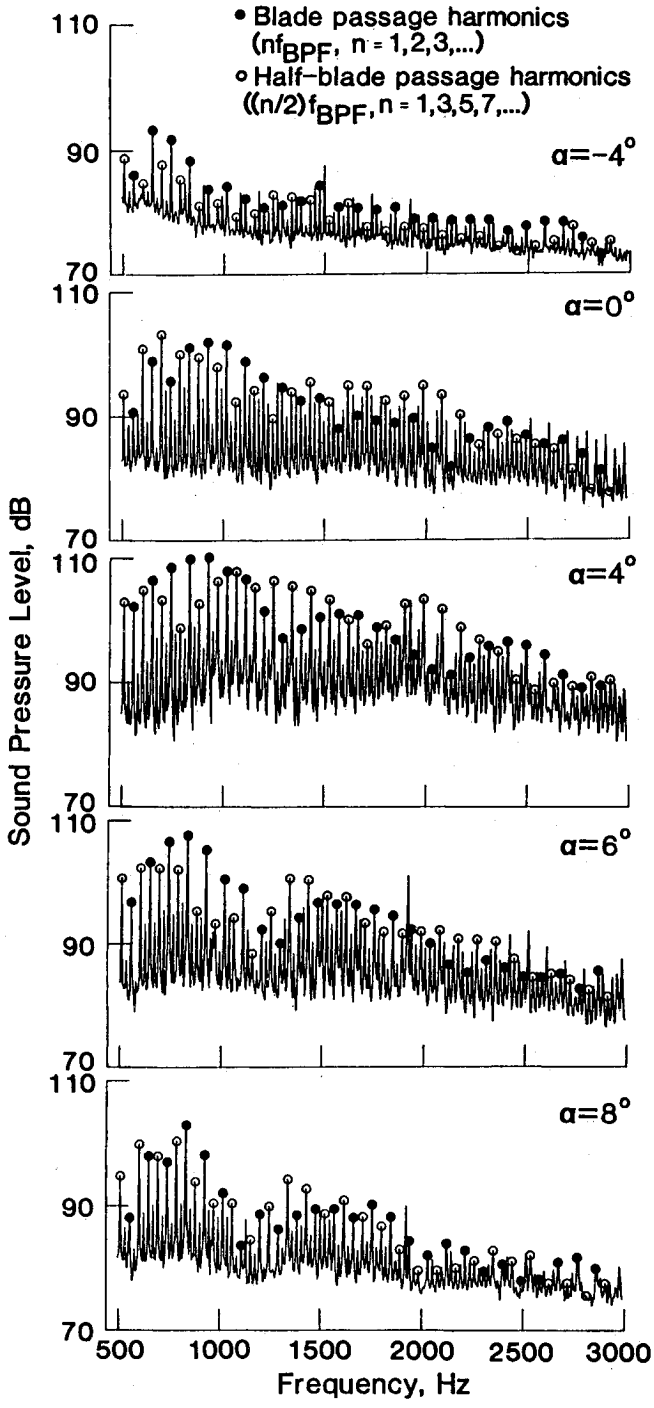

Fig. 3 Averaged narrowband spectra for tip-path-plane angles from −4 to 8 deg (50 averages, $\Delta f = 6$ Hz, $V = 70$ knots, $C_t = 0.0070$, $\mu = 0.175$, microphone 1 to Ref. 4).

and the Fourier transform

$$F(\omega) = \frac{2\pi}{P} B(\omega) \sum_{k=-\infty}^{\infty} \delta\left(\omega - \frac{2k\pi}{P}\right) \tag{3}$$

is found using the relation

$$\sum_{n=-\infty}^{\infty} e^{-i\omega nP} = \frac{2\pi}{P} \sum_{k=-\infty}^{\infty} \delta\left(\omega - \frac{2k\pi}{P}\right)$$

Substituting in $B(\omega)$ from Eq. (2), we find that

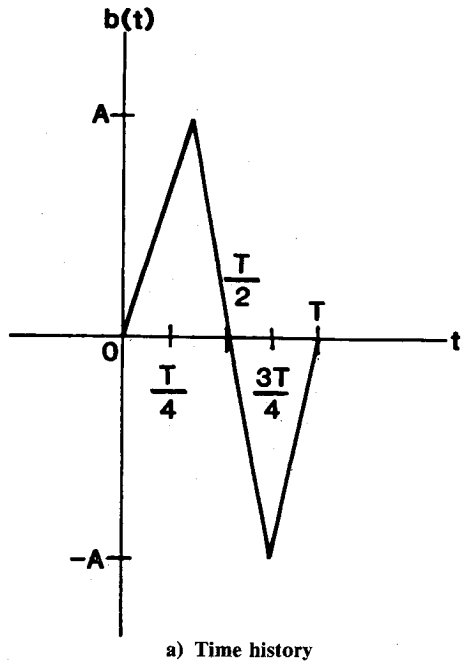

a) Time history

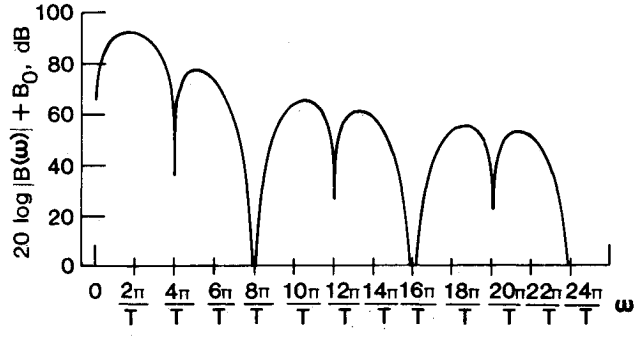

b) Magnitude of Fourier transform ($A = 1.0$, $T = 0.0013$ s)

Fig. 4 Mathematical model of simple BVI type impulse.

$$|F(\omega)| = \frac{AT}{P} \frac{\{\sin(\omega T/4)[1-\cos(\omega T/4)]\}}{(\omega T/4)^2} \times \sum_{k=-\infty}^{\infty} \delta\left(\omega - \frac{2k\pi}{P}\right) \tag{4}$$

This function is shown in Fig. 5b in decibels plus an arbitrary constant F_0. This is essentially the same scalloped spectrum of Eq. (2), but filtered by a comb function whose interval is directly related to the repetition time P of the impulse. This spectrum has power only at frequencies that are multiples of $2\pi/P$. The maxima of the spectral humps are governed by AT/P and the decay rate by $1/\omega^2$.

It is interesting to consider the decay of the spectral maxima of Eq. (4). Since the numerator of Eq. (4) is purely trigonometric, the decay rate of the spectrum is controlled by the ω^2 term in the denominator and thus is approximately 12 dB/octave. Table 1 presents the decay of the spectral maxima in terms of decibels relative to the first maximum (located near $\omega = 2\pi/T$). From this computation, it can be seen that the BVI spectral energy is primarily observed in the first four spectral maxima, or out to $\omega \simeq 14\pi/T$, where the amplitude envelope is

30 dB down from the first maximum level.

Although the spectrum of Eq. (4) exhibits many of the features of the measured spectra, it was observed that the measured spectra also contain power at the half- and quarter-harmonics of the blade passage frequency or, equivalently, at harmonics of the rotor rotation frequency. Even though the spectra are highly resolved, only those frequencies contain appreciable power. This suggests that the rotor signal is not periodic at the blade passage period P, but rather at the rotor shaft period $4P$. Certainly, dramatic blade-to-blade differences in the BVI impulses can be observed in the data of Fig. 2.

In order to model this phenomenon within the spirit of the previous analysis, let $x(t)$ be the BVI signal during one shaft revolution as shown in Fig. 6a. During this time interval there will be four blade/vortex interactions. Each of these will be modeled by the characteristic signature given by Eq. (1), but with each having their own amplitude, phase, and time interval, i.e.,

$$x(t) = \sum_{k=1}^{4} b_k'(t)$$

where

$$b_k'(t) = 0 \qquad \text{for } 0 < t < \phi_k$$

$$= \frac{4A_k}{T_k}(t-\phi_k) \qquad \text{for } \phi_k < t < \left(\frac{T_k}{4}+\phi_k\right)$$

$$= \frac{4A_k}{T_k}\left(\frac{T_k}{2}-t-\phi_k\right)$$

$$\text{for } \left(\frac{T_k}{4}+\phi_k\right) < t < \left(\frac{3T_k}{4}+\phi_k\right)$$

$$= \frac{4A_k}{T_k}(t-\phi_k-T_k)$$

$$\text{for } \left(\frac{3T_k}{4}+\phi_k\right) < t < \left(\frac{T_k}{4}+\phi_k\right)$$

$$= 0 \qquad \text{for } t > (T_k+\phi_k)$$

The Fourier transform of this signal is

$$X(\omega) = \sum_{k=1}^{4} e^{-i\omega\phi_k} B_k'(\omega)$$

where

$$B_k'(\omega) = \frac{iA_kT_k}{2\pi} e^{\frac{-i\omega Tk}{2}} \left\{\frac{\sin(\omega T_k/4)\,[1-\cos(\omega T_k/4)]}{(\omega T_k/4)^2}\right\}$$

If $x(t)$ is then supposed to repeat periodically with period $4P$, a repetition of the analysis which led to Eq. (4) yields

$$F(\omega) = \frac{2\pi}{P} X(\omega) \sum_{k=-\infty}^{\infty} \delta\left(\omega - \frac{2k\pi}{4P}\right)$$

as the Fourier transform of the periodic signal. This spectrum is similar to that given by Eq. (4), with the exception that it contains power only at multiples of the shaft rotation frequency, not at harmonics of the blade passage frequency. In addition, the amplitude envelope of the total spectrum $F(\omega)$ is the sum of the four individual scalloped spectra $B_k'(\omega)$, which are governed by A_k and T_k. An illustration of the shapes of the spectra of $B_k'(\omega)$ for four unique combinations of A_k and T_k at $P=1$ is given in Fig. 6b. The total spectrum $F(\omega)$ in decibels is shown in Fig. 6c. This spectrum still exhibits the characteristic humped shape and has power only at the shaft harmonics.

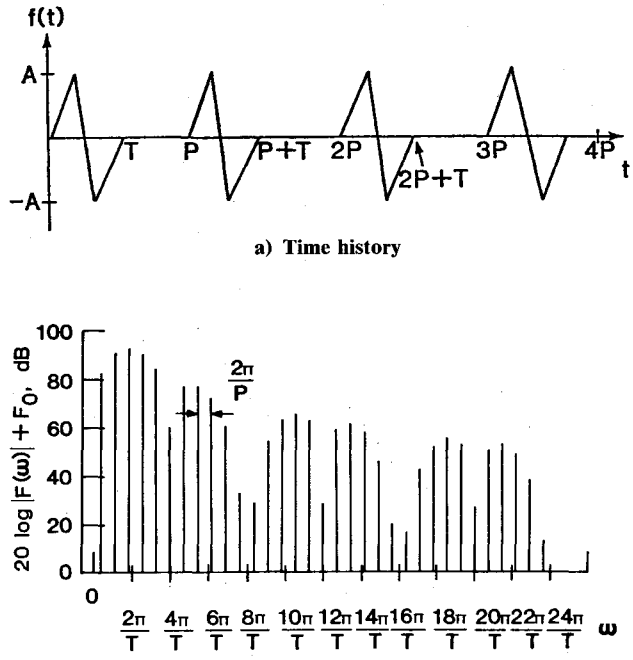

a) Time history

b) Magnitude of Fourier transform ($A=1.0$, $P=1.0$, $T=0.0013$ s)

Fig. 5 Mathematical model of periodic BVI type impulse for a four-bladed rotor.

Table 1 Estimated BVI spectral maximum amplitudes

Approximate center frequency of spectral maxima, rad/s	Amplitude relative to first maximum, dB
$2\pi/T$	0
$6\pi/T$	−14.5
$10\pi/T$	−26.9
$14\pi/T$	−30.9
$18\pi/T$	−36.7
$22\pi/T$	−39.1
$26\pi/T$	−43.0
$30\pi/T$	−44.6
$34\pi/T$	−47.5
$38\pi/T$	−48.8

Comparison of Experimental and Analytic Results

The mathematical model has shown that a typical BVI impulse signal creates a humped spectrum, with the center frequencies of the maxima related to the impulse emission time, windowed by a comb function whose line spacing is related to the impulse repetition time. The amplitudes of the spectral maxima are defined by the impulse amplitude and emission time. The decay rate of the spectral maxima can be estimated from Eq. (2) and is governed by the function $1/\omega^2$. Thus, the theory can aid in interpreting the measured time signals and power spectra.

From the theory, we can estimate that the spectral hump center frequency is equal to the inverse of the impulse emission time T. The approximate range of the center frequency of the first hump observed in the data is between 750 and 1000 Hz. The inverse of this frequency is a time length T of 0.0010–0.0013 s, which normalized by the rotor rotation period (0.0435s) corresponds to a nondimensionalized time of 0.023–0.030 of a rotor revolution. The acoustic pressure plots of Fig. 4 (at 4 deg tip-path-plane angle, for example) show that the characteristic impulse emission times range from 0.025–0.035

of a rotor revolution. Thus, the impulse emission time estimated from the first spectral hump is in reasonable agreement with the time history data.

We can also infer the periodicity or repetition time of the impulses from the midfrequency spectral line spacing. If the pulses were all identical, only the blade passage frequency harmonics would be observed. However, if each blade produces its own characteristic impulsive signal, multiples of the shaft rotation frequency (one-quarter of the blade passage frequency) appear in the spectrum. The appearance of high power at these frequencies in the data suggests that blade/vortex interaction is an unsteady process.

Conclusions

The BVI impulsive content of the acoustic signal of a model rotor is shown to appear in the midfrequency range of the power spectrum, typically between the 5th and 30th harmonics of the blade passage frequency. These harmonics exhibit a humped or scalloped shape in this midfrequency spectral region. The most acoustic energy is concentrated in the harmonics of the blade passage frequency, although a significant amount is also located at the half-blade-passage harmonics and at harmonics of the shaft frequency. Comparisons of averaged and instantaneous acoustic signals show that the BVI impulsive content can demonstrate significant unsteadiness and blade-to-blade differences.

A mathematical model of a generalized BVI acoustic signal and its power spectrum is developed to aid in interpreting the observed spectral characteristics. The model shows that the power spectrum of the generalized impulsive signal is a scalloped spectrum which is filtered by a comb function. The amplitude envelope of the spectrum is defined by the impulse amplitude and emission time. The scalloping, or humping, of the spectrum is related to the emission time of the impulse and the spacing of the comb function is related to the repetition time (period) of the impulse. The decay rate of the spectral humps is governed by the inverse of the frequency squared. The simple model also shows that increased unsteadiness and blade-to-blade differences in the impulsive signals will spread the acoustic energy from the blade passage frequency harmonics to the shaft harmonics. The results of the mathematical model illustrate the characteristics observed in the measured power spectra and indicate that these characteristics are due to blade/vortex interaction activity.

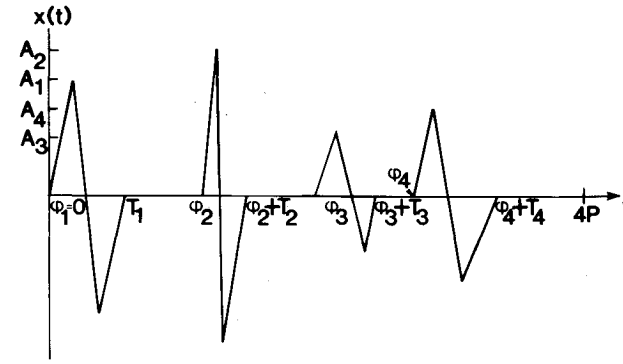

a) Time history

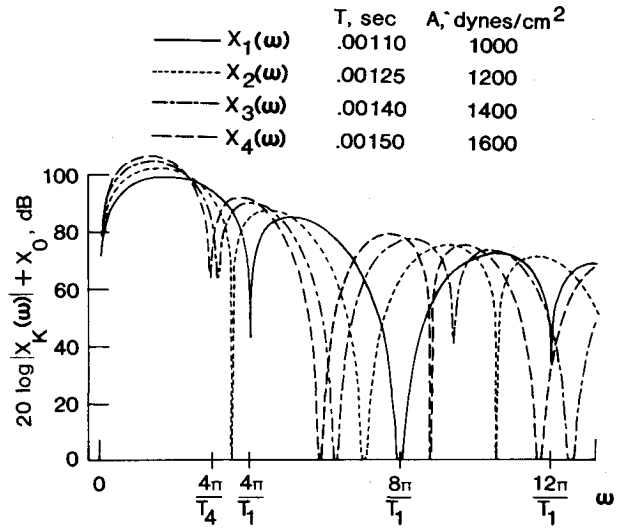

b) Amplitude envelopes of the Fourier transforms for the four individual impulses of Fig. 6a ($P = 1.0$)

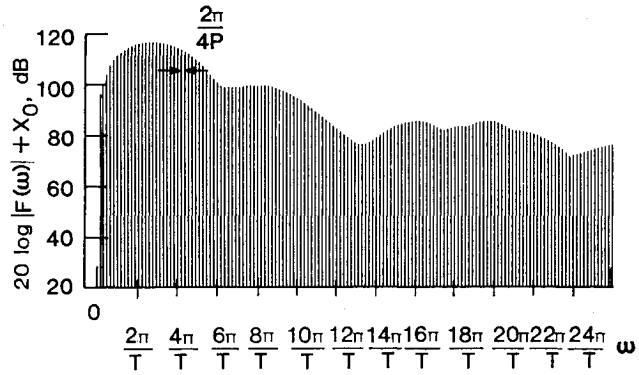

c) Magnitude of Fourier transform of total signal of Fig. 6a

Fig. 6 Mathematical model of periodic impulse for a four-bladed rotor with "blade-to-blade" differences in impulse amplitude, phase, and emission time.

References

[1]Widnall, S.E. and Wolf, T.L., "Effect of Tip Vortex Structure on Helicopter Noise Due to Blade-Vortex Interaction," *Journal of Aircraft,* Vol. 17, Oct. 1980, pp. 705-711.

[2]Hoad, D.R., "Evaluation of Helicopter Noise Due to Blade-Vortex Interaction for Five Tip Configurations," NASA TP 1608, Dec. 1979.

[3]Janakiram, D.S., "Experimental Evaluation of Active and Passive Means of Alleviating Rotor Impulsive Noise in Descent Flight," NASA CR-159188, Nov. 1979.

[4]Martin, R.M. and Connor, A.B., "Wind-Tunnel Acoustic Results of Two Rotor Models with Several Tip Designs," NASA TM 87698, July 1986.

[5]Leverton, J.W. and Amor, C.B., "An Investigation of Impulsive Rotor Noise of a Model Rotor," *Journal of Sound and Vibration,* Vol. 28, No. 1, 1973, pp. 55-77.

[6]Boxwell, D.A. and Schmitz, F.H., "Full-Scale Measurements of Blade-Vortex Interaction Noise," *Journal of the American Helicopter Society,* Vol. 27, No. 4, Oct. 1982.

[7]Boxwell, D.A. and Schmitz, F.H., "In-Flight Acoustic Comparison of the 540 and K747 Main Rotors for the AH-1S Helicopter," Appendix to U.S. Army Aviation Engineering Flight Activity Report, Project 77-38, Oct. 1979.

[8]Sternfeld, H. Jr., "Influence of the Tip Vortex on Helicopter Rotor Noise," AGARD CP 22, Sept. 1967.

[9]Widnall, S., "Helicopter Noise Due to Blade-Vortex Interaction," *Journal of the Acoustical Society of America,* Vol. 50, No. 1, Pt. 2, July 1970, pp. 354-365.

[10]Leverton, J.W. and Taylor, F.W., "Helicopter Blade Slap," *Journal of Sound and Vibration,* Vol. 4, No. 3, Aug. 1965, pp. 345-357.

[11]Schmitz, F.H. and Boxwell, D.A., "In-Flight Far-Field Measurement of Helicopter Impulsive Noise," Paper presented at 32nd Annual National V/STOL Forum of the American Helicopter Society, May 1976.

[12]Hoad, D.R., Elliott, J.W., and Orie, N.M., "Rotor Performance Characteristics from an Aeroacoustic Helicopter Wind Tunnel Test Program," NASA TM 87661, 1986.

[13]Martin, R.M., Elliott, J.W., and Hoad, D.R., "Comparison of Experimental and Analytical Predictions of Rotor Blade-Vortex Interactions Using Model Scale Acoustic Data," AIAA Paper 84-2269, Oct. 1984.

[14]Shenoy, K.R., "The Role of Scale Models in the Design of 'Low BVI Noise' Rotorcraft," *41st Annual Forum Proceedings,* American Helicopter Society, 1985, pp. 239–248.

[15]Martin, R.M. and Burley, C.L., "Power Cepstrum Technique with Application to Model Helicopter Acoustic Data," NASA TP 2586, 1986.